

X-ray Polarimetry of the accreting pulsar 1A 0535+262 in the supercritical state with PolarLight

XIANGYUN LONG,¹ HUA FENG,² HONG LI,² LING-DA KONG,³ JEREMY HEYL,⁴ LONG JI,⁵ LIAN TAO,⁶ FABIO MULERI,⁷ QIONG WU,¹ JIAHUAN ZHU,² JIAHUI HUANG,¹ MASSIMO MINUTI,⁸ WEICHUN JIANG,⁶ SAVERIO CITRARO,⁸ HIKMAT NASIMI,⁸ JIANDONG YU,⁹ GE JIN,¹⁰ MING ZENG,¹ PENG AN,⁹ LUCA BALDINI,⁸ RONALDO BELLAZZINI,⁸ ALESSANDRO BREZ,⁸ LUCA LATRONICO,¹¹ CARMELO SGRO,⁸ GLORIA SPANDRE,⁸ MICHELE PINCHERA,⁸ PAOLO SOFFITTA,⁷ AND ENRICO COSTA⁷

¹*Department of Engineering Physics, Tsinghua University, Beijing 100084, China*

²*Department of Astronomy, Tsinghua University, Beijing 100084, China*

³*Institut für Astronomie und Astrophysik, Kepler Center for Astro and Particle Physics, Eberhard Karls, Universität, Sand 1, D-72076 Tübingen, Germany*

⁴*Department of Physics and Astronomy, University of British Columbia, Vancouver, BC V6T 1Z1, Canada*

⁵*School of Physics and Astronomy, Sun Yat-Sen University, Zhuhai, 519082, China*

⁶*Key Laboratory for Particle Astrophysics, Institute of High Energy Physics, Chinese Academy of Sciences, Beijing 100049, China*

⁷*IAPS/INAF, Via Fosso del Cavaliere 100, 00133 Rome, Italy*

⁸*INFN-Pisa, Largo B. Pontecorvo 3, 56127 Pisa, Italy*

⁹*School of Electronic and Information Engineering, Ningbo University of Technology, Ningbo, Zhejiang 315211, China*

¹⁰*North Night Vision Technology Co., Ltd., Nanjing 211106, China*

¹¹*INFN, Sezione di Torino, Via Pietro Giuria 1, I-10125 Torino, Italy*

ABSTRACT

The X-ray pulsar 1A 0535+262 exhibited a giant outburst in 2020, offering us a unique opportunity for X-ray polarimetry of an accreting pulsar in the supercritical state. Measurement with PolarLight yielded a non-detection in 3–8 keV; the 99% upper limit of the polarization fraction (PF) is found to be 0.34 averaged over spin phases, or 0.51 based on the rotating vector model. No useful constraint can be placed with phase resolved polarimetry. These upper limits are lower than a previous theoretical prediction of 0.6–0.8, but consistent with those found in other accreting pulsars, like Her X-1, Cen X-3, 4U 1626–67, and GRO J1008–57, which were in the subcritical state, or at least not confidently in the supercritical state, during the polarization measurements. Our results suggest that the relatively low PF seen in accreting pulsars cannot be attributed to the source not being in the supercritical state, but could be a general feature.

1. INTRODUCTION

Accreting X-ray pulsars are powered by mass accretion onto strongly magnetized neutron stars (for a review see [Mushukov & Tsygankov 2022](#)). The high magnetic pressure truncates the accretion flow at a large radius and forces the accreting materials to fall onto the star surface along magnetic field lines. When the accretion rate or luminosity is higher than a critical value, the accretion flow will be significantly slowed down by radiation pressure above the star surface, forming radiation dominated shocks and an accretion column ([Basko & Sunyaev 1976](#)). In this supercritical state, the emission is argued to escape in form of a fan beam ([Becker & Wolff 2007](#)).

Caiazzo & Heyl (2021) calculated the X-ray polarization signature for luminous accreting pulsars based on the accretion column model described in [Becker & Wolff \(2007\)](#), suggesting that the geometry of the system can be inferred via phase resolved polarimetry. They predicted a polarization

fraction (PF) as high as 0.6–0.8 generally. However, Observations of Her X-1 with the Imaging X-ray Polarimetry Explorer (IXPE) detected a PF of only about 0.05–0.15 over spin phases, far below the theoretical prediction ([Doroshenko et al. 2022](#)). The authors proposed several possible scenarios to account for the discrepancy, including one that questions the presence of the accretion column, because Her X-1 displays a positive correlation between the cyclotron line energy and luminosity ([Staubert et al. 2014](#)), indicating that the source is in the subcritical state. Cen X-3 is the second accreting pulsar observed with IXPE, which made a non-detection in its low state and measured a similar level of polarization in a bright state, with a PF of 0.05–0.15 as a function of spin phase ([Tsygankov et al. 2022](#)). It is uncertain whether the source is in the sub or supercritical state, as the cyclotron line energy does not vary as a function of luminosity ([Bachhar et al. 2022](#); [Yang et al. 2023](#)); the X-ray luminosity during detection also gives an ambiguous determination ([Becker et al. 2012](#); [Mushukov et al. 2015](#)). Later, a non-detection was obtained with an IXPE measurement of 4U 1626–67, a persistent ultracompact low-mass X-ray pulsar, at a subcritical luminosity ([Marshall et al. 2022](#)). Recently, a similar polarization signature with PF varying

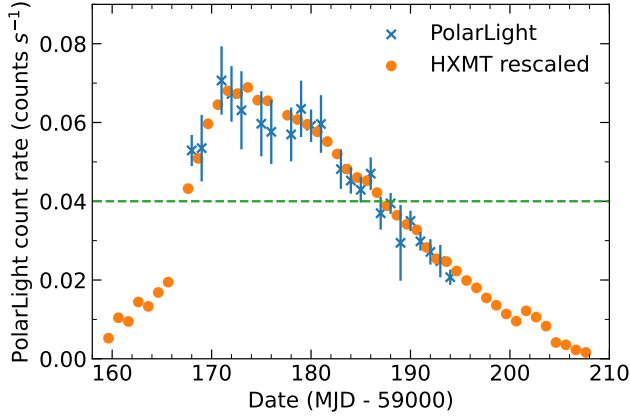


Figure 1. One-day averaged 3–8 keV X-ray lightcurves of 1A 0535+262 during the 2020 major outburst measured with PolarLight (blue) and HXMT (orange; rescaled to match the PolarLight flux). The error bar has a size of 1σ for PolarLight and is smaller than the symbol for HXMT. The horizontal dashed line marks the level above which the source was in the supercritical state (Kong et al. 2021).

around 0.1 with spin phase is seen in a transient Be/X-ray binary pulsar GRO J1008–57 during its subcritical outburst in late 2022 (Tsygankov et al. 2023).

Thus, it would be interesting to measure X-ray polarization from a source in a *bona fide* supercritical state, as a direct test to argue for or against this scenario. The 2020 giant burst (Kong et al. 2021, 2022; Ma et al. 2022; Wang et al. 2022; Chhotaray et al. 2023) from the transient Be/X-ray binary pulsar 1A 0535+262 offered us such an opportunity and was observed with the X-ray polarimeter PolarLight (Feng et al. 2019). The outburst is the most luminous one known so far for this source and reached a peak luminosity of $1.2 \times 10^{38} \text{ erg s}^{-1}$ (Kong et al. 2021). Observations with Insight-HXMT (Zhang et al. 2020) revealed that the source transitioned into the supercritical state, where the cyclotron absorption line energy is negatively correlated with luminosity, above the critical luminosity of $6.7 \times 10^{37} \text{ erg s}^{-1}$ (Kong et al. 2021). The PolarLight observations cover the supercritical cycle. In this paper, we present the polarimetric results in this state and try to address the above question.

2. OBSERVATIONS AND ANALYSIS

PolarLight is an X-ray polarimeter onboard a CubeSat (Feng et al. 2019), to measure X-ray polarization using the gas pixel detector, a 2D position sensitive proportional counter (Bellazzini et al. 2013; Li et al. 2015). It was launched in October 2018 into a Sun synchronous orbit for technical demonstration (Li et al. 2021) and preliminary science observations (Feng et al. 2020; Long et al. 2021, 2022). PolarLight observed 1A 0535+262 from November 15 to December 12, 2020, with a total effective exposure of 69 ks. The emission state and pulsar ephemeris are adopted from HXMT observations with obsIDs P0304099001-18 and P0314316001-15 (Kong et al. 2021, 2022; Hou et al. 2023);

details about the HXMT data reduction can be found in Kong et al. (2021). The lightcurves of the outburst measured with the two instruments are displayed in Figure 1. The supercritical state ranges from MJD 59167 to 59187, during which there are 33 ks of PolarLight observations in total. In this work, we focus on the analysis of this part of data.

The energy calibration for PolarLight is implemented by comparing the observed energy spectrum with a simulated one, given the best-fit spectral model obtained with HXMT (Kong et al. 2021). With a phenomenological energy spectrum as an input, we simulate the measured spectrum with the Geant4 package and find the detector gain by comparing it with the measured spectrum. This technique has been justified in previous observations (Feng et al. 2020; Li et al. 2021; Long et al. 2021, 2022). Events located in the central $\pm 7 \text{ mm}$ region with an image spreading over at least 58 pixels are selected for polarimetric analysis. We employ an energy-dependent algorithm (Zhu et al. 2021) to discriminate the background events. The Stokes parameters are used to calculate the polarization (Kislat et al. 2015; Mikhalev 2018), and the intrinsic PF and polarization angle (PA) are inferred using a Bayesian approach to remove the bias in the estimate (Maier et al. 2014; Mikhalev 2018). The peak location on the marginalized posterior distribution is adopted as the point estimate, and the credible interval (the highest density interval from the same distribution) is adopted as the error.

We calculated the X-ray polarization in different energy bands and always got a non-detection. We thus adopted the energy band of 3–8 keV to report the result; consistent results can be obtained in other bands with larger uncertainties. In this energy band, the mean polarization modulation factor (μ) is 0.42 weighted by the measured X-ray energies, and the residual background after discrimination has a fraction of 6.8% averaged over the supercritical state. Given the number of detected photons from the source (n_s) and background (n_b), the minimum detectable polarization at 99% confidence level ($\text{MDP}_{99} = \frac{4.29}{\mu n_s} \sqrt{n_s + n_b}$; Weisskopf et al. 2010) is 0.27.

In the energy band of 3–8 keV and during the supercritical state, the spin phase averaged polarization measurement gives $\text{PF} = 0.12^{+0.13}_{-0.12}$ (90% C. L.), indicative of a non-detection. We thus do not quote the measured PA. The 90%, 99%, and 99.73% upper limit on the PF is 0.25, 0.34, and 0.38, respectively. The modulation curve is displayed in Figure 2 for visual inspection. The PA vs. PF posterior distribution is shown in Figure 3.

The PolarLight data alone do not allow us to find the pulsar spin period and fold the lightcurve. We thereby rely on the ephemeris computed with HXMT observations (Kong et al. 2022; Hou et al. 2023). Both the barycentric correction and binary motion are taken into account. The mean spin period is roughly 103.5 s and varies slowly during the outburst. Therefore, for non-simultaneous observations, we extrapolated the HXMT result from the closest epoch, typically with a time separation of 0.2–0.5 d. The pulse profiles averaged over the supercritical state measured with the two instruments are shown in Figure 4.

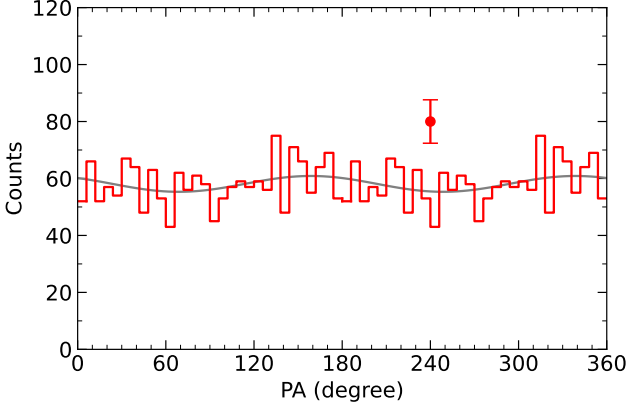


Figure 2. Spin phase averaged polarimetric modulation curve of 1A 0535+262 measured with PolarLight over the supercritical state. The vertical bar indicates a typical 1σ error. The gray line is the model curves derived from the Stokes/Bayesian analysis.

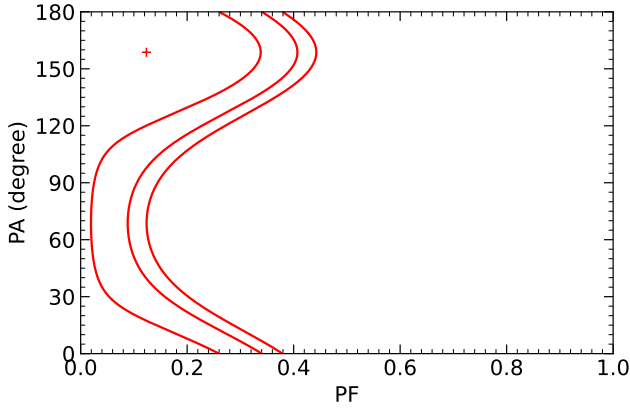


Figure 3. Spin phase averaged PA vs. PF contours of 1A 0535+262 measured with PolarLight over the supercritical state. The cross indicates the point estimate and the contours encircle the 90%, 99%, and 99.73% credible intervals of the Bayesian posterior distribution.

We calculated the polarization at different phases. Limited by the number of photons, we chose a phase bin size of 0.25 and shift the bin center at a step of 0.01. Again, we had non-detections at any central phases; the highest detection significance is only 2.6σ . The PF upper limits as well as MDP_{99} at different central phases are also displayed in Figure 4. As a result of small number of photons in a phase bin, the upper limits are not constraining.

We then fit the PolarLight data with a rotating vector model (RVM; Radhakrishnan & Cooke 1969; Poutanen 2020) using an unbinned likelihood analysis method (González-Caniulef et al. 2023). This is to assume that the PA is determined by the magnetic axis of the pulsar and modulated on the sky plane by pulsar spin. Even with the presence of vacuum birefringence due to strong magnetic fields, in which case the polarization is determined by the field lines at the limiting radius far from the star surface, the RVM is still applicable

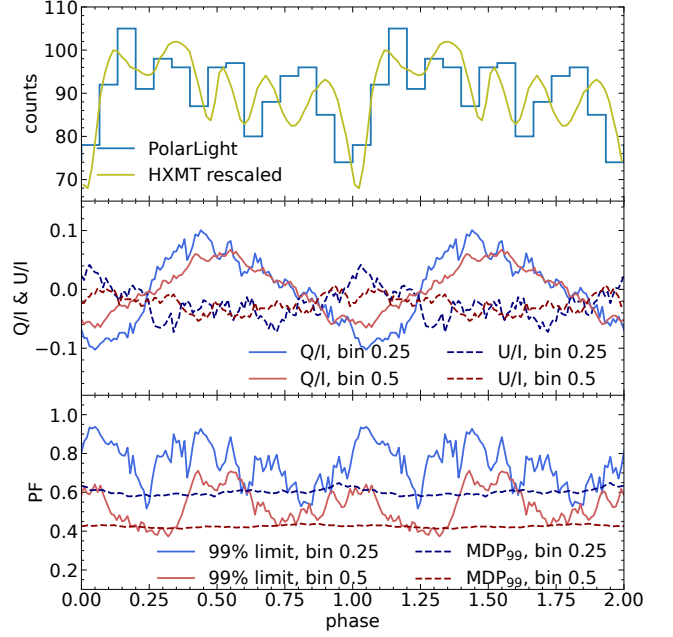


Figure 4. Spin phase resolved polarimetry of 1A 0535+262 over the supercritical state in the 3–8 keV energy range. **Top:** folded pulse profiles using the ephemeris constructed with HXMT. **Middle:** normalized Stokes Q and U parameters as a function of phase. **Bottom:** MDP_{99} and the 99% PF upper limit as a function of phase. The polarimetric parameters are calculated by moving a phase bin with a size of 0.25 and 0.5, respectively, at a step of 0.01.

if the bipolar field is the dominant component at that radius (Heyl & Shaviv 2000). In fact, the RVM model has been successfully used to model the phase dependent PA variation in several X-ray accreting pulsars (Doroshenko et al. 2022; Tsygankov et al. 2022, 2023). In addition to PF, the model contains the phase zeropoint ϕ_0 and 3 parameters for the pulsar geometry: inclination of the spin axis to the line of sight i_p , magnetic obliquity θ , and the spin axis projected on the sky plane χ_p (see Fig. 4 in Doroshenko et al. 2022). We assume uniform priors, PF and ϕ_0 in 0–1, i_p and χ_p in 0–180°, and θ in 0–90°. With Markov Chain Monte Carlo simulations, the 90%, 99%, and 99.73% upper limits on the PF are inferred to be 0.41, 0.51, and 0.57, respectively. The posterior distributions of the parameters are shown in Figure 5. Taking into account the large uncertainties, the inferred i_p deviates from the binary inclination angle by 2σ (88^{+31}_{-28} vs. 35° ; Giovannelli et al. 2007), and the inferred θ is in line with the magnetic obliquity derived from pulse profile modeling (45^{+17}_{-13} vs. 50°) that assumes an inclination $i_p = 35^\circ$ (Caballero et al. 2011; Hu et al. 2023). If we fix i_p at 35° , the constraint on θ is even worse. We want to emphasize that the apparent agreement is mainly because of the larger errors from our fits as a result of non-detection. Thus, we do not further discuss the geometries to avoid over-interpretation, but focus on the PF upper limit.

3. DISCUSSION

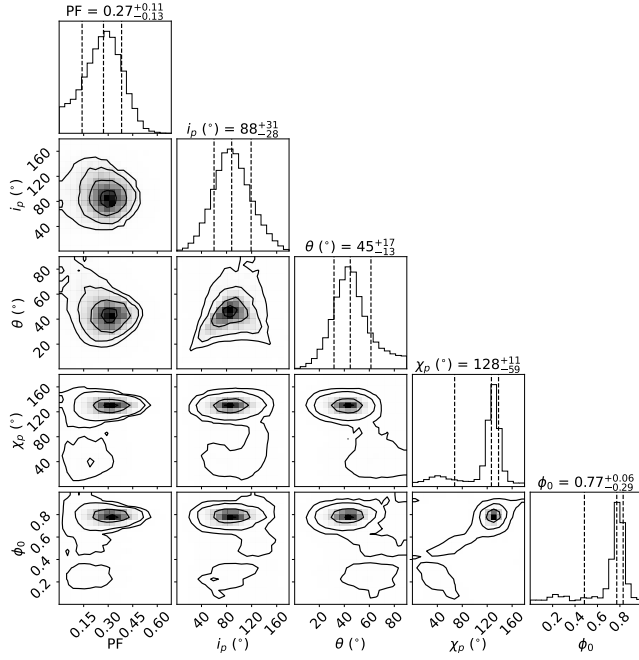


Figure 5. Corner plot of the posterior distributions for the parameters in the RVM model, which assumes a constant polarization modulated by the spin of pulsar. The errors are quoted at 68% credible level.

We present X-ray polarimetric results of the accreting pulsar 1A 0535+262 during the supercritical state. Measurements with PolarLight yielded a non-detection in 3–8 keV with a phase averaged PF upper limit of 0.34 at 99% credible level. Due to the small area of PolarLight, the phase resolved polarimetry leads to loose constraints; we cannot rule out that the source has high PFs in some spin phase ranges. Based on the RVM with a constant PF, we obtained a 99% PF upper limit of 0.51.

According to previous IXPE measurements, the RVM was always able to fit the data adequately (Doroshenko et al. 2022; Marshall et al. 2022; Tsygankov et al. 2022, 2023). Here, based on the RVM, we are unsure if the intrinsic PF of the source is higher than those derived in other sources,

but it is indeed lower than the theoretical prediction of 0.6–0.8 (Caiazzo & Heyl 2021), suggesting that the relatively low PFs measured in Her X-1 (Doroshenko et al. 2022), Cen X-3 (Tsygankov et al. 2022), 4U 1626–67 (Marshall et al. 2022), and GRO J1008–57 (Tsygankov et al. 2023) cannot be attributed to the sources not being in the supercritical state. One may consider other possibilities for relatively low polarizations as proposed by Doroshenko et al. (2022) and Tsygankov et al. (2022), including mode conversion due to vacuum resonance in the emitting plasma with a strong temperature gradient (Pavlov & Shibanov 1979; Lai & Ho 2002; Doroshenko et al. 2022), the quasi-tangential effect occurred during radiation transfer (Wang & Lai 2009; Caiazzo & Heyl 2021), and reflection/scattering on the ambient surface or medium (Tsygankov et al. 2022). To further investigate this problem, joint spectroscopy, timing, and polarimetry are needed for a large sample of accreting pulsars; this can be accomplished with the future enhanced X-ray Timing and Polarimetry (eXTP) observatory (Zhang et al. 2019).

We note that 1A 0535+262 and GRO J1008–57 are transient Be/X-ray binaries (Reig 2011), while Her X-1 and Cen X-3 are persistent sources; Her X-1 contains an intermediate mass companion (Middleditch & Nelson 1976) and Cen X-3 contains a massive supergiant companion (Hutchings et al. 1979). 4U 1626–67 is a transient in an ultracompact binary with an extremely low mass companion (Middleditch et al. 1981). All these imply that a relatively low PF in accreting pulsars could be a general feature, independent on their companion type, accretion mode, or luminosity.

We thank the anonymous referee for useful comments. We acknowledge funding support from the National Key R&D Project under grant 2018YFA0404502, the National Natural Science Foundation of China under grants Nos. 12025301, 12103027, 11821303, & 12122306. HF acknowledges the Tsinghua University Initiative Scientific Research Program. LT acknowledges the CAS Pioneer Hundred Talent Program Y8291130K2.

Facility: PolarLight, HXMT

REFERENCES

- Bachhar, R., Raman, G., Bhalerao, V., & Bhattacharya, D. 2022, MNRAS, 517, 4138, doi: [10.1093/mnras/stac2901](https://doi.org/10.1093/mnras/stac2901)
- Basko, M. M., & Sunyaev, R. A. 1976, MNRAS, 175, 395, doi: [10.1093/mnras/175.2.395](https://doi.org/10.1093/mnras/175.2.395)
- Becker, P. A., & Wolff, M. T. 2007, ApJ, 654, 435, doi: [10.1086/509108](https://doi.org/10.1086/509108)
- Becker, P. A., Klochov, D., Schönherr, G., et al. 2012, A&A, 544, A123, doi: [10.1051/0004-6361/201219065](https://doi.org/10.1051/0004-6361/201219065)
- Bellazzini, R., Brez, A., Costa, E., et al. 2013, Nuclear Instruments and Methods in Physics Research A, 720, 173, doi: [10.1016/j.nima.2012.12.006](https://doi.org/10.1016/j.nima.2012.12.006)
- Caballero, I., Kraus, U., Santangelo, A., Sasaki, M., & Kretschmar, P. 2011, A&A, 526, A131, doi: [10.1051/0004-6361/201014728](https://doi.org/10.1051/0004-6361/201014728)
- Caiazzo, I., & Heyl, J. 2021, MNRAS, 501, 109, doi: [10.1093/mnras/staa3428](https://doi.org/10.1093/mnras/staa3428)
- Chhotaray, B., Jaisawal, G. K., Kumari, N., et al. 2023, MNRAS, 518, 5089, doi: [10.1093/mnras/stac3354](https://doi.org/10.1093/mnras/stac3354)
- Doroshenko, V., Poutanen, J., Tsygankov, S. S., et al. 2022, Nature Astronomy, 6, 1433, doi: [10.1038/s41550-022-01799-5](https://doi.org/10.1038/s41550-022-01799-5)
- Feng, H., Jiang, W., Minuti, M., et al. 2019, Experimental Astronomy, 47, 225, doi: [10.1007/s10686-019-09625-z](https://doi.org/10.1007/s10686-019-09625-z)

- Feng, H., Li, H., Long, X., et al. 2020, *Nature Astronomy*, 4, 511, doi: [10.1038/s41550-020-1088-1](https://doi.org/10.1038/s41550-020-1088-1)
- Giovannelli, F., Bernabei, S., Rossi, C., & Sabau-Graziati, L. 2007, *A&A*, 475, 651, doi: [10.1051/0004-6361:20066149](https://doi.org/10.1051/0004-6361:20066149)
- González-Caniulef, D., Caiazzo, I., & Heyl, J. 2023, *MNRAS*, 519, 5902, doi: [10.1093/mnras/stad033](https://doi.org/10.1093/mnras/stad033)
- Heyl, J. S., & Shaviv, N. J. 2000, *MNRAS*, 311, 555, doi: [10.1046/j.1365-8711.2000.03076.x](https://doi.org/10.1046/j.1365-8711.2000.03076.x)
- Hou, X., Zhang, W., Torres, D. F., Ji, L., & Li, J. 2023, *ApJ*, 944, 57, doi: [10.3847/1538-4357/acaec7](https://doi.org/10.3847/1538-4357/acaec7)
- Hu, Y. F., Ji, L., Yu, C., et al. 2023, *ApJ*, 945, 138, doi: [10.3847/1538-4357/acbc7a](https://doi.org/10.3847/1538-4357/acbc7a)
- Hutchings, J. B., Cowley, A. P., Crampton, D., van Paradijs, J., & White, N. E. 1979, *ApJ*, 229, 1079, doi: [10.1086/157042](https://doi.org/10.1086/157042)
- Kislat, F., Clark, B., Beilicke, M., & Krawczynski, H. 2015, *Astroparticle Physics*, 68, 45, doi: [10.1016/j.astropartphys.2015.02.007](https://doi.org/10.1016/j.astropartphys.2015.02.007)
- Kong, L. D., Zhang, S., Ji, L., et al. 2021, *ApJL*, 917, L38, doi: [10.3847/2041-8213/ac1ad3](https://doi.org/10.3847/2041-8213/ac1ad3)
- Kong, L.-D., Zhang, S., Ji, L., et al. 2022, *ApJ*, 932, 106, doi: [10.3847/1538-4357/ac6e66](https://doi.org/10.3847/1538-4357/ac6e66)
- Lai, D., & Ho, W. C. G. 2002, *ApJ*, 566, 373, doi: [10.1086/338074](https://doi.org/10.1086/338074)
- Li, H., Feng, H., Muleri, F., et al. 2015, *Nuclear Instruments and Methods in Physics Research A*, 804, 155, doi: [10.1016/j.nima.2015.09.060](https://doi.org/10.1016/j.nima.2015.09.060)
- Li, H., Long, X., Feng, H., et al. 2021, *Advances in Space Research*, 67, 708, doi: [10.1016/j.asr.2020.09.001](https://doi.org/10.1016/j.asr.2020.09.001)
- Long, X., Feng, H., Li, H., et al. 2021, *ApJL*, 912, L28, doi: [10.3847/2041-8213/abfb00](https://doi.org/10.3847/2041-8213/abfb00)
- , 2022, *ApJL*, 924, L13, doi: [10.3847/2041-8213/ac4673](https://doi.org/10.3847/2041-8213/ac4673)
- Ma, R., Tao, L., Zhang, S.-N., et al. 2022, *MNRAS*, 517, 1988, doi: [10.1093/mnras/stac2768](https://doi.org/10.1093/mnras/stac2768)
- Maier, D., Tenzer, C., & Santangelo, A. 2014, *PASP*, 126, 459, doi: [10.1086/676820](https://doi.org/10.1086/676820)
- Marshall, H. L., Ng, M., Rogantini, D., et al. 2022, *ApJ*, 940, 70, doi: [10.3847/1538-4357/ac98c2](https://doi.org/10.3847/1538-4357/ac98c2)
- Middleditch, J., Mason, K. O., Nelson, J. E., & White, N. E. 1981, *ApJ*, 244, 1001, doi: [10.1086/158772](https://doi.org/10.1086/158772)
- Middleditch, J., & Nelson, J. 1976, *ApJ*, 208, 567, doi: [10.1086/154638](https://doi.org/10.1086/154638)
- Mikhalev, V. 2018, *A&A*, 615, A54, doi: [10.1051/0004-6361/201731971](https://doi.org/10.1051/0004-6361/201731971)
- Mushtukov, A., & Tsygankov, S. 2022, *arXiv e-prints*, arXiv:2204.14185, doi: [10.48550/arXiv.2204.14185](https://doi.org/10.48550/arXiv.2204.14185)
- Mushtukov, A. A., Suleimanov, V. F., Tsygankov, S. S., & Poutanen, J. 2015, *MNRAS*, 447, 1847, doi: [10.1093/mnras/stu2484](https://doi.org/10.1093/mnras/stu2484)
- Pavlov, G. G., & Shibano, I. A. 1979, *Zhurnal Eksperimentalnoi i Teoreticheskoi Fiziki*, 76, 1457
- Poutanen, J. 2020, *A&A*, 641, A166, doi: [10.1051/0004-6361/202038689](https://doi.org/10.1051/0004-6361/202038689)
- Radhakrishnan, V., & Cooke, D. J. 1969, *Astrophys. Lett.*, 3, 225
- Reig, P. 2011, *Ap&SS*, 332, 1, doi: [10.1007/s10509-010-0575-8](https://doi.org/10.1007/s10509-010-0575-8)
- Staubert, R., Klochkov, D., Wilms, J., et al. 2014, *A&A*, 572, A119, doi: [10.1051/0004-6361/201424203](https://doi.org/10.1051/0004-6361/201424203)
- Tsygankov, S. S., Doroshenko, V., Poutanen, J., et al. 2022, *ApJL*, 941, L14, doi: [10.3847/2041-8213/aca486](https://doi.org/10.3847/2041-8213/aca486)
- Tsygankov, S. S., Doroshenko, V., Mushtukov, A. A., et al. 2023, *arXiv e-prints*, arXiv:2302.06680, doi: [10.48550/arXiv.2302.06680](https://doi.org/10.48550/arXiv.2302.06680)
- Wang, C., & Lai, D. 2009, *MNRAS*, 398, 515, doi: [10.1111/j.1365-2966.2009.14895.x](https://doi.org/10.1111/j.1365-2966.2009.14895.x)
- Wang, P. J., Kong, L. D., Zhang, S., et al. 2022, *ApJ*, 935, 125, doi: [10.3847/1538-4357/ac8230](https://doi.org/10.3847/1538-4357/ac8230)
- Weisskopf, M. C., Elsner, R. F., & O'Dell, S. L. 2010, in *Society of Photo-Optical Instrumentation Engineers (SPIE) Conference Series*, Vol. 7732, *Space Telescopes and Instrumentation 2010: Ultraviolet to Gamma Ray*, ed. M. Arnaud, S. S. Murray, & T. Takahashi, 77320E, doi: [10.1117/12.857357](https://doi.org/10.1117/12.857357)
- Yang, W., Wang, W., Liu, Q., et al. 2023, *MNRAS*, 519, 5402, doi: [10.1093/mnras/stad048](https://doi.org/10.1093/mnras/stad048)
- Zhang, S., Santangelo, A., Feroci, M., et al. 2019, *Science China Physics, Mechanics, and Astronomy*, 62, 29502, doi: [10.1007/s11433-018-9309-2](https://doi.org/10.1007/s11433-018-9309-2)
- Zhang, S.-N., Li, T., Lu, F., et al. 2020, *Science China Physics, Mechanics, and Astronomy*, 63, 249502, doi: [10.1007/s11433-019-1432-6](https://doi.org/10.1007/s11433-019-1432-6)
- Zhu, J., Li, H., Feng, H., et al. 2021, *Research in Astronomy and Astrophysics*, 21, 233, doi: [10.1088/1674-4527/21/9/233](https://doi.org/10.1088/1674-4527/21/9/233)